

Evaluating the Carbon Cycle of a coupled Atmosphere-Biosphere Model

C. Delire, J. A. Foley, S. Thompson

This article was submitted to
American Geophysical Union 2002 Fall Meeting, San Francisco,
CA., December 7-10, 2002

U.S. Department of Energy

August 21, 2002

Lawrence
Livermore
National
Laboratory

DISCLAIMER

This document was prepared as an account of work sponsored by an agency of the United States Government. Neither the United States Government nor the University of California nor any of their employees, makes any warranty, express or implied, or assumes any legal liability or responsibility for the accuracy, completeness, or usefulness of any information, apparatus, product, or process disclosed, or represents that its use would not infringe privately owned rights. Reference herein to any specific commercial product, process, or service by trade name, trademark, manufacturer, or otherwise, does not necessarily constitute or imply its endorsement, recommendation, or favoring by the United States Government or the University of California. The views and opinions of authors expressed herein do not necessarily state or reflect those of the United States Government or the University of California, and shall not be used for advertising or product endorsement purposes.

This is a preprint of a paper intended for publication in a journal or proceedings. Since changes may be made before publication, this preprint is made available with the understanding that it will not be cited or reproduced without the permission of the author.

This work was performed under the auspices of the United States Department of Energy by the University of California, Lawrence Livermore National Laboratory under contract No. W-7405-Eng-48.

This report has been reproduced directly from the best available copy.

Available electronically at <http://www.doc.gov/bridge>

Available for a processing fee to U.S. Department of Energy
And its contractors in paper from
U.S. Department of Energy
Office of Scientific and Technical Information
P.O. Box 62
Oak Ridge, TN 37831-0062
Telephone: (865) 576-8401
Facsimile: (865) 576-5728
E-mail: reports@adonis.osti.gov

Available for the sale to the public from
U.S. Department of Commerce
National Technical Information Service
5285 Port Royal Road
Springfield, VA 22161
Telephone: (800) 553-6847
Facsimile: (703) 605-6900
E-mail: orders@ntis.fedworld.gov
Online ordering: <http://www.ntis.gov/ordering.htm>

OR

Lawrence Livermore National Laboratory
Technical Information Department's Digital Library
<http://www.llnl.gov/tid/Library.html>

Evaluating the carbon cycle of a coupled atmosphere-biosphere model.

Christine Delire¹, Jonathan A. Foley¹, and Starley Thompson²

1. Center for Sustainability and the Global Environment (SAGE), Gaylord Nelson Institute for Environmental Studies, University of Wisconsin, 1710 University Avenue, Madison, WI 53726

2. Lawrence Livermore National Laboratory, L-103, 7000 East Avenue Livermore, CA 94550-9234

For submission to Global Biogeochemical Cycles

Revised version: August 2002

Contact: Christine Delire

Address: SAGE, University of Wisconsin, 1710 University Avenue, Madison, WI 53726

Phone: 1-608-262-5961

Fax: 1-608-265-4113

Abstract

We investigate how well a coupled biosphere-atmosphere model, CCM3-IBIS, can simulate the functioning of the terrestrial biosphere and the carbon cycling through it. The simulated climate is compared to observations, while the vegetation cover and the carbon cycle are compared to an offline version of the biosphere model IBIS forced with observed climatic variables. The simulated climate presents some local biases that strongly affect the vegetation (e.g., a misrepresentation of the African monsoon). Compared to the offline model, the coupled model simulates well the globally averaged carbon fluxes and vegetation pools. The zonal mean carbon fluxes and the zonal mean seasonal cycle are also well represented except between 0° and 20°N due to the misrepresentation of the African monsoon. These results suggest that, despite regional biases in climate and ecosystem simulations, this coupled atmosphere-biosphere model can be used to explore geographic and temporal variations in the global carbon cycle.

1. Introduction

Emissions of carbon dioxide (CO₂) from fossil fuel combustion and land use practices are increasing the atmospheric CO₂ concentration and affecting the Earth's radiation balance and climate. The continental biosphere and the oceans currently absorb about half of the anthropogenic CO₂ emissions, but this rate of uptake depends on the functioning of the biosphere and the oceans, which in turn depend on the climate and the atmospheric CO₂ concentration. To predict future changes in CO₂ concentration and climate, it is necessary to take into account the potential feedbacks between atmospheric CO₂ concentration, climate and carbon exchange between the atmosphere, oceans and

biosphere. Therefore, climate models should include explicit representations of the global carbon cycle – including the interactions between atmospheric, oceanic, and terrestrial carbon pools.

Two recent modeling studies [*Cox et al.*, 2000; *Friedlingstein et al.*, 2001], using very different model configurations, suggest that biospheric and oceanic carbon uptake could be significantly reduced by future climate change. However, their results differ in the magnitude of the biospheric signal. In *Cox et al.*, the biospheric uptake is reduced to zero and the biosphere becomes a net source of carbon, enhancing the CO₂ increase due to anthropogenic activity, while in *Friedlingstein et al.*, the uptake is reduced but the biosphere remains a net sink of carbon.

These contrasting results raise the question of how well a terrestrial biosphere model coupled to a general circulation model (GCM) can simulate the carbon cycle in the first place. GCMs effectively simulate the large-scale average seasonal distribution of pressure, temperature, circulation, and extratropical precipitation but their skill at simulating regional climates is low [*Gates*, 1995]. Do those biases in the regional climate allow for a reasonable simulation of the functioning of the biosphere? Here, we try to answer this question with a coupled biosphere-atmosphere model: the terrestrial ecosystem/land-surface model IBIS [*Kucharik et al.*, 2000] coupled to the NCAR CCM3 [*Kiehl et al.*, 1998].

There have been a number of modeling studies of the carbon exchange between the terrestrial biosphere and the atmosphere either with fluxes simulated by land surface models directly coupled to a GCM or advected with a transport model (e.g. *Fung* [1987], *Knorr* [1995]; *Denning* [1996], *Nemry* [1996], see *Craig* [1998] for an exhaustive list).

These studies focused on the short-term exchange of carbon and employed land surface models that did not represent vegetation dynamics or changing carbon pools. Our study builds on this research by representing the full dynamic carbon cycling in the vegetation and soil.

We present here the mean carbon cycle simulated by the coupled biosphere-atmosphere model CCM3-IBIS at the end of a long (350 year) run with fixed sea-surface temperatures. The interannual variability and the long-term variability of the vegetation and the carbon cycle will be discussed in subsequent papers.

2. IBIS-2: Model Description

In this study, we use an updated version of the Integrated Biosphere Simulator (IBIS) of Foley et al. [1996] and Kucharik et al. [2000]. IBIS (version 2) is a comprehensive model of terrestrial biospheric processes, and includes land-surface physics, canopy physiology, plant phenology, vegetation dynamics and competition, and carbon cycling.

The IBIS land surface module simulates the energy, water, carbon, and momentum balance of the soil-vegetation-atmosphere system on a short timestep consistent with GCMs (~20 to 60 minutes). The land surface module borrows much of its basic structure from the LSX land surface package [Thompson and Pollard, 1995a; Thompson and Pollard, 1995b]. The module includes two vegetation layers (i.e., “trees” and “grasses and shrubs”) and six soil layers to simulate soil temperature, soil water, and soil ice content over a total depth of 4 m. Physiologically-based formulations of C_3 and C_4 photosynthesis [Farquhar et al., 1980], stomatal conductance [Collatz et al., 1992;

Collatz et al., 1991] and respiration [*Amthor*, 1984] are used to simulate canopy gas exchange processes. This approach provides a mechanistic link between the exchange of energy, water, and CO₂ between vegetation canopies and the atmosphere. Budburst and senescence depend on climatic factors following the empirical algorithm presented by [*Botta et al.*, 2000].

The annual carbon balance allows the vegetation dynamics sub-model to predict the maximum leaf area index and biomass for 12 plant functional types (pfts), which compete for light and water. IBIS represents vegetation dynamics using very simple competition rules. The relative abundance of the 12 pfts in each gridcell changes in time according to their ability to photosynthesize and use water. For example, in a gridcell where trees and grasses coexist, grasses are shaded by trees and receive less light but their rooting profile allows them to withdraw water first as it infiltrates through the soil. In drought conditions, grasses will be favored, trees will accumulate less carbon, will grow less leaves and eventually wilt. Competition between grass types or between tree types result from different allocation, phenology, type of leaf, or type of photosynthesis leading to different annual carbon balances.

IBIS simulates carbon cycling through the vegetation, litter and soil organic matter (Figure 1). The soil biogeochemistry module is similar to the CENTURY model [*Parton et al.*, 1993] and the biogeochemistry model of Verberne [1990]. The total belowground carbon in the first meter of soil is divided into pools characterized by their residence time: from a few hours for the microbial biomass to more than 1000 years for stabilized organic matter. Decomposition rates of litter and soil carbon depend on soil temperature and soil moisture.

IBIS has been extensively tested against site-specific biophysical measurements from flux towers [Delire and Foley, 1999] as well as spatially extensive ecological [Kucharik et al., 2000] and hydrological data [Lenters et al., 2000].

IBIS is explicitly designed to work within atmospheric models and has been extensively used in both uncoupled (e.g., [Foley et al., 1996; Kucharik et al., 2000]) and coupled modes (e.g., [Foley et al., 2000; Foley et al., 1998; Levis et al., 1999a; Levis et al., 1999b; Levis et al., 1999c; Levis et al., 2000]).

3. Simulations and data sets used.

We performed two simulations: one in which IBIS was coupled to the NCAR CCM3 atmospheric model [Kiehl et al., 1998] and one in which was IBIS forced with observed climate data for the 20th century. In this way, we can isolate the biases due to the terrestrial ecosystem model IBIS only, due to the atmospheric model CCM3 and due to the interaction between the vegetation and the atmosphere. Biases due to the offline model IBIS alone have been described in an earlier paper [Kucharik et al., 2000] and will not be emphasized here.

In this study, the coupled model CCM3-IBIS is run for 300-year at a resolution of T31 (the spectral representation of the horizontal fields is truncated at the 31st wavenumber using a triangular truncation. Horizontal fields are converted to a $\sim 3.75^\circ \times 3.75^\circ$ grid). Fixed climatological sea surface temperatures (SSTs) are used. The T31 resolution offers an acceptable compromise between computing costs and accuracy of the simulated climate. To limit computing costs, we accelerate the vegetation dynamics

module so that it achieves 150 years during 20 years of actual atmospheric model simulation.

The off-line version of IBIS is run at the same spatial resolution over 500 years. We use the monthly dataset of temperature, precipitation, relative humidity, and cloudiness from 1901 to 1995 compiled by New [2000] (referred to as CRU05) as forcing to the offline model. To run our simulation over 500 years, we interpolate the data at the GCM T31 resolution, construct a de-trended 60-year climate record (from 1936 to 1995), and repeated this sequence eight times. We use this historical dataset instead of a climatological dataset to represent the interannual variability of the current climate.

The soil texture dataset used in the coupled model CCM3-IBIS and IBIS off-line is the IGBP-DIS global gridded texture database (International Geosphere-Biosphere Programme - Data and Information System (IGBP-DIS) 1999) interpolated at the T31 resolution. Both simulations are initialized with an 'observed' potential vegetation map [Ramankutty and Foley, 1999] and run with a constant CO₂ concentration of 350 ppmv, characteristic of the mid 1980s. Because the soil carbon has a very long characteristic timescale, we accelerate the soil carbon module in both runs so that the soil carbon achieves 3500 years during the 100 first years of the run.

In order to compare the results from the coupled model to the results of the offline model, we average the last 60 years of each run.

4. Simulated Climate

The vegetation distribution and the carbon balance simulated by the coupled model CCM3-IBIS depend strongly on the simulated climate. Therefore, we first

compare the simulated climate to observations from the CRU05 dataset. We then analyze the simulated vegetation structure and composition and the simulated carbon cycle by comparing results from the coupled model CCM3-IBIS with results from IBIS off-line and direct observations when available.

Here, we focus on near surface air temperature and precipitation because they are the most important climate variables for the vegetation. The climate simulated by the coupled model CCM3-IBIS with a prescribed vegetation map is discussed in detail in an earlier paper [Delire *et al.*, in press June 2002]. The climate simulated here is not identical to the simulated climate described in Delire *et al.* In the latter, the coupled model was run with a prescribed vegetation map so that the simulated climate did not affect the composition and structure of the vegetation. Here, the simulated climate affects vegetation structure and composition, which in turn influence the climate. The differences between the two simulated climates are therefore due to dynamic vegetation feedbacks. In the following discussion, we point out the biases in the simulated climate and try to distinguish between purely atmospheric model causes and dynamic vegetation feedback causes.

In boreal winter (December, January, February), the coupled model tends to underestimate surface temperature on the continents around the North Atlantic, and overestimate temperature both south of the Laurentian Lakes in Canada and in a narrow region stretching from the Caspian Sea to Northern Siberia (Figure 2, a). This pattern of cold and warm bias in the Northern hemisphere was also noted in studies where CCM3 was coupled to other land-surface models: LSM and a simple bucket type land-surface module [Bonan, 1998; Delire *et al.*, in press June 2002]. Therefore, it is likely that the

atmospheric model (or the sea-surface temperatures) is responsible for these biases. Temperatures are also too high in Argentina and along the Andes. The latter is mostly due to the flattened topography of the Andes in the model at low spatial resolution.

In boreal summer (June, July, August), the coupled model simulates lower than observed temperatures in Alaska and Northern Siberia (Figure 2, b). This cold bias is about 2° C stronger than in Delire et al. indicating a feedback of the vegetation. The lower than observed temperatures simulated by the atmospheric model favors tundra at the expense of forests in these regions. Tundra has a higher albedo than boreal forest especially in spring when snow is present, and absorbs less energy. Temperature is decreased in spring, melting is delayed which results in colder summer conditions. Greenland, USA and eastern Canada, the Andes, and a stretch of land North of the Mediterranean Sea from Spain to Lake Baikal are too warm. The lack of lakes, wetlands and crops in CCM3-IBIS partly explains the warm bias in North America [Delire et al., in press June 2002]. The warm bias in the Andes is again due to the poor representation of the steep orography of the Andes in the fairly low resolution coupled model. The high temperatures in Greenland are partly due to the snow module in CCM3-IBIS.

GCMs have known biases in the precipitation fields, especially in the low latitudes, resulting from inaccurate parameterization of convection and low resolution. The coupled model CCM3-IBIS overestimates precipitation on the continents: 2.50 mm/day instead of 2.08mm/day on average over all continents except Antarctica (the CRU05 dataset doesn't cover Antarctica). To a lesser extent, this was also the case with the original land surface model LSM [Bonan, 1998]. The largest errors occur in Africa and the Arabian Peninsula where the model fails to represent the location and intensity of

the West African monsoon (Figure 2 d). Instead of being located close to the Gulf of Guinea, the model simulates the African monsoon over Sudan, Ethiopia and the Arabian Peninsula where it connects with the Indian monsoon. As a result, summers are too dry in West Africa and too wet in northeastern Sahel, and from the Arabian Peninsula to central India (JJA). This misrepresentation of the west-African monsoon was also obtained with CCM3 coupled to another land-surface model, LSM [Bonan, 1998], and is likely related to the atmospheric model. The fairly low resolution used here accentuates the problem. The effect of vegetation dynamics on this bias is minor. In central and South Africa, maximum precipitation is too high during the wet season (DJF) and the dry season is too long.

On the other continents, there are a variety of precipitation biases. The model overestimates precipitation over the Tibetan plateau all year round, which was also the case with LSM and is due to the atmospheric model. The model strongly underestimates precipitation in Indochina and S-E China during the wet season (JJA) while Northern China, Mongolia and S-E Siberia are too wet. The model tends to exaggerate the dry season in the Indonesian Archipelago. Seasonal precipitation reaches too far south into western Australia in austral summer. In the Amazon basin in South America, precipitation is underestimated during the wet season north of the Equator (JJA) and the dry season is too long south of the Equator. The Nordeste is too wet in the wet season. Southern Brazil and the mouth of the Rio de la Plata are too dry all year round. In North America, Alaska and the Rockies are too wet in winter and spring, central Canada from Lake Winnipeg to Hudson Bay is too dry in summer and fall and South-eastern US is too dry year round. Most of the biases in the precipitation fields were obtained with LSM

coupled to the CCM3 and with CCM3-IBIS with fixed vegetation [*Delire et al.*, in press June 2002]. They are most likely due to the GCM. Vegetation feedbacks play a role but the amplitude of the feedback is smaller than the biases. In North America for instance, vegetation dynamics results in slightly dryer conditions, reducing the wet bias in the West and enhancing the drought in the East.

To analyze the simulated climate in a non-spatial way, we calculate the fraction of land area that falls within a certain annual temperature and precipitation range and compare it to observations from the CRU05 dataset (Table 1). Early work in ecology (e.g. [*Holdridge*, 1947]) or on carbon cycling in vegetation and soils ([*Lieth*, 1975; *Post et al.*, 1982]) showed that annual precipitation and annual temperature are key factors in determining the type of vegetation, net primary productivity (NPP) and soil respiration. Despite the important local biases in the simulated temperature and precipitation fields, the area of land experiencing a certain annual temperature and precipitation range is close to the observed. For instance, the coupled model simulates 9.5 % of the land cover (minus Antarctica) with annual temperatures ranging from 20°C to 30°C and mean annual precipitation from 2 to 4 mm/day. According to the CRU05 dataset, 12.7 % of the total land cover (minus Antarctica) falls within this category. The coupled model does not necessarily simulate that given ‘climate’ at the right location but does simulate it over an area comparable to the observations. GCMs are known to simulate effectively the general circulation of the atmosphere but not the exact placement of the particular atmospheric circulation patterns [*Gates*, 1995]. Here, while there are regional biases, CCM3 conserves the land areas falling within a certain annual temperature and precipitation range.

Differences in the temperature-precipitation distribution include, for instance, a higher simulated than observed fraction of land with temperature between -10 and 0 °C and precipitation greater than 2 mm/day. This is also true for the areas with annual temperatures between 0 and 10 °C. The Tibetan Plateau, where precipitation is overestimated, is mostly responsible for these differences. The GCM doesn't simulate climate regimes with annual temperatures below -20 °C (except in Antarctica, which is not included here).

5. Simulated Vegetation Cover

The performance of the off-line model in simulating the vegetation structure and composition and the carbon cycling in the biosphere was described in an earlier paper [Kucharik *et al.*, 2000]. Here, we test the performance of the coupled model CCM3-IBIS by comparing its results primarily to the results of the off-line version of IBIS and secondarily to direct observations when available. There are several reasons for adopting this approach. First, very few global gridded observations of natural vegetation cover are available. Second, the model used in the offline simulation is basically identical to the one coupled to the CCM3. By comparing both results, we can isolate biases due to the coupling to the climate model. Third, the results from the offline model are necessarily better than the results of the coupled model because the offline model is forced with observed climate data. The coupled model calculates its own climate and therefore compounds errors from both the land surface model and the climate model.

Leaf area index

In IBIS, the vegetation cover is represented in terms of 12 plant functional types (pfts) competing for light and water. The maximum leaf area index (LAI) reached during the year for each pft depends on the amount of carbon assimilated by this pft during the previous year. LAI in the model is thus linked to the carbon cycling and is therefore a good indicator of the behavior of the model. To ease the comparison between the coupled model and the offline model, we grouped the 12 pfts into evergreen trees (tropical broadleaf evergreen, warm-temperate broadleaf evergreen, temperate conifer evergreen, and boreal conifer evergreen trees), deciduous trees (tropical broadleaf drought-deciduous, temperate broadleaf cold-deciduous, boreal broadleaf cold-deciduous, and boreal conifer cold-deciduous trees), and grasses and shrubs (evergreen and cold-deciduous shrubs, C4 and C3 grasses). The total LAI for each group is simply the sum of the LAIs of the corresponding individual pfts.

Except for a stretch of land south-east of Lake Chad, the coupled model simulates lower LAIs than the off-line version around the equator where evergreen tropical trees are simulated (Figure 3,a and 4,a). Deciduous trees gain from the competition with evergreen tropical trees in the Amazon basin, central Africa and Indonesia (Figure 3, b). This change in vegetation composition results from the underestimation of the precipitation during the dry season simulated by the GCM in the tropical regions. The LAI of evergreen trees (warm temperate) is increased in South Africa and from Saudi Arabia to N-W India at the expense of grasses and shrubs and deserts (Figure 3, b, c). Temperate and boreal evergreen trees have higher LAIs over the Tibetan plateau (at the expense of grasses and shrubs), in central Asia, Siberia and in central US.

Increased precipitation allows deciduous trees to colonize the Sahel and the south of the Arabian Peninsula. Higher spring to fall rainfall also favors temperate deciduous trees S-E of Lake Baikal. In eastern US and Canada, deciduous trees lose competition in favor of C4 grasses because the lower precipitation together with the higher summer temperatures result in lower available soil moisture. Cooler summers in Alaska and Siberia explain lower LAI of deciduous trees (and conifer) trees while warmer conditions West of Hudson Bay explain higher LAI for deciduous trees.

In most of Africa, C4 grasses lose competition in favor of trees because of too wet conditions. Because of these wetter conditions, grasses are established further N in the Sahara. Wetter conditions also explain lower LAIs of grasses (replaced by trees) in China while drier conditions explain the lower LAIs in eastern Australia.

Vegetation types

Vegetation type is only a diagnostic output in IBIS but it allows easy comparison between model results. The vegetation type of a gridcell is calculated using simple rules based on the leaf area index (LAI) of the different plant functional types in that gridcell, and some overriding climatic rules. For example, a gridcell is classified as a temperate deciduous forest if temperate broadleaf cold deciduous trees have the highest LAI in that particular gridcell and if the total LAI of the upper canopy is greater than 1.5. If it is smaller than 1.5, the same gridcell is classified as a savanna. If the annual 5°C growing-degree-days (GDD5) is lower than 350, it is classified as tundra.

The offline model IBIS forced with climate observations represents well the major characteristics of today's potential vegetation, with tropical evergreen forests along the equator, surrounded by tropical deciduous forests and savannas [*Kucharik et al.*,

2000]. Grasslands and shrublands mark the transition with the deserts around the Sahara or the Gobi desert. Grassland and shrublands are simulated in the Western US and Australia, South Africa and South America. Temperate deciduous forests are simulated around the North Atlantic and the coast of China, boreal forests in Canada and North-central Eurasia and tundra in the Arctic. However, the off-line model IBIS fails to represent extensive savannas because of poor representation of disturbance in the model [Foley *et al.*, 1996] and [Kucharik *et al.*, 2000]. Savannas are known to depend on disturbances as fire or extreme weather events, neither of which are well represented in the model [Botta and Foley, June 2002, In press]. Other discrepancies include too extensive temperate evergreen forests in Argentina and overly extensive tropical deciduous forests in Africa and South America, at the expense of savannas.

The coupled model presents the same general vegetation characteristics as the offline model but some of the GCM biases in the precipitation and temperature fields together with vegetation climate feedbacks affect the simulated vegetation types. The most obvious differences are the forests simulated in the Arabian Peninsula and Iran and the boreal forest simulated on the Tibetan Plateau (Figure 4). The northern vegetation limit (*polar desert / tundra*) simulated by the coupled model CCM3-IBIS reaches higher latitudes N-W of Hudson Bay than with the off-line version but lower latitudes in northern Siberia because of the aforementioned warm bias in N Canada and the cold bias everywhere else around the N. Pole. The same pattern of warm and cold biases around the Arctic explains why the treeline is simulated further north in northern Canada, N-W of Hudson Bay and is displaced further south in Eurasia and Alaska. In these regions, the model simulates spring to fall cooler than observed temperatures resulting in values of

GDD5 (~200) lower than the limit for existence of boreal trees in the model (> 350). The warm bias in N-W Canada is more pronounced in spring than in Delire et al because the establishment of trees lowers the albedo of the surface thereby increasing the available energy.

The coupled model simulates a boreal forest over the Tibetan Plateau because of the overestimated precipitation rates. The transition between boreal and temperate forests is fairly well represented but the coupled model doesn't accurately represent the limit between boreal or temperate forests and grassland, shrubland and desert. Grasslands expand too far east in the US at the expense of deciduous forest and desert conditions are simulated around Lake Winnipeg as a downstream result of the poor representation of the orography of the Rockies. The grasslands in Eastern US are due to the high summer temperatures simulated by the GCM reducing the water availability together with the lower precipitation (Figure 2 d). On the other hand, higher precipitation rates result in temperate forests extending too far West in Eastern China at the expense of grasslands. The GCM simulates well the Sahara and the Gobi deserts but simulates desert conditions in N-E Australia, N. Burma, and Argentina.

In the tropics, Africa is the least well represented by the coupled model. The overestimated precipitation rates result in too extensive tropical and temperate forests with very little grassland and savannas.

We use the kappa statistic [*Monserud*, 1990 (Aug)] to evaluate the spatial agreement between the two vegetation distributions (Table 2). The most extreme environments – polar deserts, tropical evergreen forests and deserts - have the best spatial agreements. Mixed forests, savannas and shrublands have the poorest spatial agreement.

The largest errors in simulated total areas covered by each vegetation type (Table 2) do not necessarily coincide with the poorest spatial agreement. For instance, there is very poor spatial agreement for savannas but their simulated areas are within 9 % of each other. This relates to the similarity between simulated and observed land areas falling within a certain range of annual temperature and precipitation, as mentioned above.

6. Simulated Carbon Balance

The carbon cycle in IBIS can be separated into two main components: the vegetation and the soils (Figure 1). In each gridcell, the vegetation cover is a combination of pfts, each characterized in terms of three biomass pools: leaves, stems and fine roots. Those three biomass pools are the fundamental variables from which all the variables describing the vegetation are derived. For each plant functional type i , the rate of change in each biomass compartment j (leaf, stem or root) is given by:

$$\frac{dC_{v,i,j}}{dt} = a_{i,j}NPP_i - LF_{i,j} - D_{i,j}$$

where $a_{i,j}$ is the fraction of annual NPP allocated to each biomass compartment (leaf, wood or root), LF_{ij} indicates litterfall from each compartment and D_{ij} the disturbance (fire, wind ...). In each grid cell, the rate of change in total biomass C_v is simply the sum of the changes of each biomass compartment for each plant functional type, and the total fluxes are simply given by:

$$\begin{aligned} NPP &= \sum_{i=1}^{n_{pft}} \sum_{j=1}^3 a_{i,j}NPP_i \\ LF &= \sum_{i=1}^{n_{pft}} \sum_{j=1}^3 LF_{i,j} \\ D &= \sum_{i=1}^{n_{pft}} \sum_{j=1}^3 D_{i,j} \end{aligned}$$

Similarly, the evolution of the different soil carbon pools can be summarized as:

$$\frac{dC_s}{dt} = LF - HR - L$$

where C_s , the total carbon content in the soil is the sum of the different individual pools (microbial biomass, slow and recalcitrant carbon pools), HR represents heterotrophic respiration (microbial respiration) and L leaching of carbon through the soil column. As a whole, the carbon content in the biosphere changes according to:

$$\frac{d(C_v + C_s)}{dt} = NEE - L$$

where NEE , the net ecosystem exchange represents the net flux of carbon between the biosphere and the atmosphere and is equal to $NPP - HR - D$. We chose to count as positive any flux from the atmosphere to the biosphere. Equilibrium is reached when, averaged over several years, the carbon pools are constant, and NEE compensates exactly leaching.

Global averages of carbon fluxes and pools are similar in the coupled model and in the off-line model (Table 3). With the exception of the NEE , the total soil carbon and leaching, the fluxes and pools simulated by the two models are within 5% of each other, although the GCM has a slightly slower carbon cycle than the off-line model. Neither simulation is at equilibrium at the end of the run but the imbalances are very small: biomass increases by $.16 \text{ Gt C yr}^{-1}$ (0.2 %) and the total soil carbon content by $0.08 \text{ Gt C yr}^{-1}$ (0.005 %).

We first discuss the geographical distribution of the carbon stocks in the vegetation and soils and then the carbon fluxes.

Biomass

The distribution of living biomass is directly related to the distribution of trees and grasses, as trees accumulate more carbon than grasses. Therefore, the highest biomass values are found in the tropical and temperate forests and the lowest are found in deserts, grasslands and tundras. The coupled model overestimates biomass in comparison to the offline model on a stretch of land from Lake Chad to the S-E of Lake Baykal because of higher spring to fall precipitation (Figure 5). Overestimated precipitation in comparison to observations also explains higher biomass values in South Africa, Argentina, N-E of Brazil and in the Northern Plains of North America. Underestimated precipitation is responsible for the lower biomass in S-E China, Burma, W. Africa, Uruguay, S-E of the US (together with higher summer temperatures) and around Lake Winnipeg. Lower summer rainfall rates together with higher summer temperatures explain the lower biomass in S-E US and western Europe. The warm and cold summer bias around the Arctic explains higher values of biomass W. of Hudson Bay and lower biomass in Alaska and Siberia.

Soil carbon

As expected, soil carbon content is highest in boreal region where degradation is slow, lowest both in deserts where NPP is low and in tropical regions where degradation is fast (Figure 6). Simulated values range from 0 kg C m⁻² in deserts to a maximum of 51 kg C m⁻² in Northern Canada with the coupled model and to a maximum of 44 kg C m⁻² in the off-line version. Observed values from the IGBP-DIS (Scholes [1995], IGBP-DIS [1999]) soil database range from 0 to 85 kg C m⁻². The coupled model simulates 20% more carbon in the soil than the offline version. The coupled model simulates larger soil carbon contents in the Northern latitudes, on the Tibetan Plateau, in Africa, and from the

Arabian Peninsula through central India. The higher values in the tropics, the Tibetan Plateau and Northern Canada are explained by a higher NPP not fully compensated by higher respiration rates. The higher values around the Arctic, which account for 60 % of the difference in total soil carbon content, can't be explained by the values of the carbon fluxes (NPP and heterotrophic respiration) over the last 60 years of the run. They partly result from the high (350 ppmv) atmospheric CO₂ concentration imposed for the length of the run and the acceleration technique used. Because of the acceleration of the soil carbon module, the soil carbon pool has actually experienced 3000 years with 350 ppmv instead of the 280 ppmv prevalent during the last 2000 years. The high CO₂ concentration is more likely to affect the arctic regions because the slow decomposition rates result in very long residence times.. Lower soil carbon contents are simulated in eastern US and at the mouth of the Rio de la Plata.

We compare biome averages and standard deviations of simulated and observed soil carbon from the IGBP-DIS dataset (Figure 7). The averages and standard deviations for the observed data are obtained by assigning each grid cell to the corresponding offline IBIS vegetation type for that gridcell. Soil carbon contents agree fairly well for most of the vegetation types. Mixed forests, open shrublands, tundra and polar deserts and deserts present the largest discrepancies between models and observations. One possible explanation for the observed high values in the deserts might be the result of previous climate conditions (warmer and wetter conditions during the Holocene) not simulated with the model and could also be related to the small number of pedons available to construct the dataset (6 in Mali, 2 in Oman, and 3 in Australia). The high values

simulated for the tundra are linked to the aforementioned acceleration technique and the 350 ppmv atmospheric CO₂ concentration imposed.

Net primary productivity

Over the last 60 years of the run, the global annual average net primary productivity (NPP) estimated by the coupled model is 54.3 Gt C yr⁻¹ with an interannual variability (estimated by the standard deviation) of 0.9 Gt C yr⁻¹. In the offline version of the model, the 60-year average is 54.5 Gt C yr⁻¹ with a standard deviation of 1.6 GtC yr⁻¹. Both values are within 5% of each other and fall within the range of 44 – 66 Pg yr⁻¹ [Cramer *et al.*, 1999] obtained with other (offline) models. Because we use fixed sea-surface temperatures, the interannual variability of temperature and precipitation simulated by the coupled model is smaller than the observed variability of the climate, explaining the reduced standard deviation in NPP. Locally, NPP varies from 0 in deserts to a maximum of 1.3 kg m⁻² yr⁻¹ in tropical forests. The differences in the geographical distribution of NPP simulated by the coupled model and the offline model (not shown) follows closely the biases in spring to fall precipitation except in the Arctic where the differences in NPP are related to the temperature biases.

Total NPP as a function of latitude is at a maximum around the equator, and a minimum around 20N because of the Sahara desert (Figure 8). The coupled model simulates similar total NPPs, except for a lower maximum around the equator. This is due to slightly lower NPP of the tropical evergreen forest caused by the exaggerate dry season and a higher minimum around 20N explained by the greener Sahel and Arabian Peninsula. Cooler than observed summers explain the lower NPP at high northern latitudes.

We compare the net primary productivity (aboveground and belowground) averaged per vegetation types simulated by the coupled model and IBIS offline with a compilation of field measurements (unpublished data, Gower) (Figure 9). This data set combines data from Esser [1997], [Cannell, 1982] and Gower (unpublished data). The 1882 points were assembled in the 15 IBIS vegetation types by [Kucharik *et al.*, 2000] to evaluate the offline version of IBIS at a $1^{\circ}\times 1^{\circ}$ resolution. Belowground productivity is estimated using [Gower *et al.*, 1999] ratio of belowground to aboveground NPP. For both the observations and the models, the error bars indicate the standard deviation among the different values of NPP for the same vegetation type. We don't expect model results to match exactly the observations. The model simulates a gridcell average of NPP while field studies are generally made on small plots. However, the model values need to fall within the range of measured values (shown by the error bars). The offline IBIS and the coupled model CCM3-IBIS tend to underestimate tropical and temperate forest NPPs. Both models strongly underestimate grassland and shrubland NPP. There is much less scatter in the simulated values of NPP for each vegetation type than in the observations. This can be partly explained by the resolution used in the models: topography, soils and climate are homogenous over a 3.75-degree gridcell not representative of the spatial variability in reality.

Heterotrophic respiration

The global annual average heterotrophic respiration simulated by the coupled model over the last 60 years is $47.6 \text{ Gt C yr}^{-1}$, 71 % of the total soil carbon flux ($67.7 \text{ Gt C yr}^{-1}$). Root respiration accounts for 29 % of the total soil carbon flux. The offline model simulates slightly higher values of the heterotrophic respiration and the total soil carbon

flux (48.7 and 70.8 Gt C yr⁻¹) coherent with the simulated higher productivity. Locally, total soil CO₂ fluxes vary from 0 to 1.55 kg C m⁻² yr⁻¹ in the coupled model (0 to 1.789 kg C m⁻² yr⁻¹ in the offline model) and follow the general patterns of NPP.

The latitudinal distribution of yearly heterotrophic respiration follows closely the patterns of NPP (Figure 8). This behavior is expected because both simulations are run towards equilibrium for which $NPP - HR - D - L = 0$ and because the remaining fluxes, disturbance (D) and leaching (L) are small.

Seasonality of the carbon fluxes.

Dargaville et al (submitted to GBC) tested the performance of the offline IBIS and 3 other models in simulating the seasonal cycle of the carbon fluxes using an atmospheric transport model and observations of atmospheric CO₂. They showed that the offline IBIS (and to a lesser extent the other models) tends to underestimate the amplitude of the seasonal cycle of the net ecosystem exchange in the Northern Hemisphere. The coupled model gives similar results as the offline version in the northern-most latitudes (60-90N) and in the southern hemisphere between 0 and 30 S (Figure 10 and 11). Both models simulate similar seasonal cycles for NPP and heterotrophic respiration, which result in similar seasonality of NEE. In the northern mid-latitudes, the coupled model simulates a stronger seasonal cycle than the offline model due to a stronger seasonality in the NPP. NPP increases too fast in spring reaches a maximum in May-June and decreases too early (July). Too early and excessive growth in spring in China and Siberia S-E of Lake Baikal due to wetter conditions explains the higher NPPs in spring. Excessive temperatures and limited water availability in summer in eastern US explain the early drop in NPP. In the low latitudes of the Northern hemisphere (0-30N), the coupled model

underestimates the amplitude of the seasonal cycle of NEE. The misrepresentation of the West African monsoon connecting with the Indian monsoon is responsible for this discrepancy between the results of the 2 models. When the Arabian Peninsula, Ethiopia, Sudan and Egypt are removed from the computation of total NEE, the seasonal cycle simulated by the GCM is within 10 % of the seasonal cycle simulated by the offline model.

7. Summary and conclusions

In this paper, we investigate how well a coupled biosphere-atmosphere model can simulate carbon cycling and the general functioning of the terrestrial biosphere. Therefore, we analyze the climate, vegetation cover and carbon cycle in the vegetation and soils simulated by a coupled atmosphere-biosphere CCM3-IBIS. The climate is compared to observations, while the vegetation cover and the carbon cycle are compared to an offline version of IBIS forced with observed climatic variable. The comparison of the simulated climate to an earlier simulation with the coupled model where the vegetation is fixed [Delire *et al.*, in press June 2002] shows that the biases in the simulated climate are mainly due to the atmospheric model. The coupling with the vegetation dynamics enhances or reduces some of those biases but, the effect is small compared to the magnitude of the biases.

As already mentioned, GCMs do not accurately simulate local and regional climates but their skill at simulating the large-scale distribution of pressure, temperature, circulation, and precipitation is high. This is clearly the case with CCM3-IBIS. The coupled model simulates a geographic distribution of the temperature and precipitation

fields that presents important local biases like the high precipitation in the Arabian Peninsula but the area of land experiencing certain ranges of annual temperature and precipitation are similar to observations. As a result, the simulated vegetation cover presents local anomalies like the deciduous forest in Saudi-Arabia but the total area covered by each vegetation type (except grasslands) simulated by the coupled model is similar to the area simulated by the offline model. The geographic distribution of the carbon fluxes and pools presents important local differences but with the exception of the soil carbon content, the global averages are almost identical, indicating that the coupled model simulates a biosphere that functions, on the whole, in a manner similar to the offline model forced with climatic observations.

The zonal mean of the annual carbon fluxes is affected by the local biases in the simulated climate, but the differences do not exceed $0.5 \text{ Gt C year}^{-1}$, except between 10 and 20 degree N (Sahel and Arabia) where they reach 1 Gt C year^{-1} . This means that the biases in the fluxes compensate each other zonally, except for the latitude band of the Sahel. The seasonality of the zonally averaged carbon fluxes is well represented in the coupled model in comparison to the offline model, although there are major flaws between 0 and 30 °N due to the misrepresentation of the African monsoon.

Averaged per vegetation types, the carbon fluxes are very similar indicating that the vegetation types simulated by the GCM function in the same way as the vegetation types simulated by the offline model, even if their exact location is not always correct.

The biases in the simulated regional climates do not affect the vegetation in the same way. Biases in winter temperatures, for example, play a less important role than biases during the growing season. On the other hand, the patterns of warm and cold

biases in summer around the Arctic strongly influence the northern vegetation limit and the northern treeline. The warm summer bias together with the precipitation in the eastern US affect vegetation cover and carbon fluxes and pools. This bias also affects the seasonality of the zonal mean flux by reducing the NPP too early in summer.

The most important bias in the simulated precipitation field is the misrepresentation of the African monsoon extending to central India. It dramatically affects the vegetation cover in the Sahel, the Arabian Peninsula and from the Persian Gulf to India. It also strongly affects the seasonality of the zonal mean fluxes. The excessive precipitation over the Tibetan Plateau results in boreal forest instead of tundra, but this does not affect the zonal mean of the annual carbon fluxes and their seasonal cycle. On the other hand, the excess summer precipitation SE of Lake Baykal affects strongly the seasonality of the carbon fluxes of that latitude band. The exaggerated dry season in the tropical forests is responsible for slightly lower NPPs and a higher percentage of tropical deciduous trees.

In summary, despite some important biases in the simulated local climate and carbon fluxes and pools, the coupled model simulates a biosphere functioning as a whole in a similar way than the offline model. Global values of carbon pools and fluxes are almost identical. Zonal averages and averages per vegetation types are very similar. The seasonality of the zonal carbon fluxes is also well reproduced, except for the 0-30N latitude band.

In this study, the atmospheric CO₂ concentration was kept fixed to 350 ppmv not allowing vegetation and soils to affect it. This limitation is justified by the absence of an interactive ocean model. CCM3-IBIS is now coupled to an ocean carbon cycling model

in order to simulate the full carbon cycle and the effect of fossil fuel emissions on the functioning of the atmosphere-biosphere-ocean system.

According to our study, coupled models can be used to explore the global, hemispheric and zonal-mean coupling of atmospheric and terrestrial carbon cycles. This is compatible with the level of observational detail now available from flask measurements and inverse modeling studies. Further regional detail (at particular regions) will require further improvements in the fidelity of climate simulations, as well as regional data, not yet available.

This work has also some implications for the strategy of future coupled model development. Coupling of models improves their capacity at reproducing the real processes but the results of the coupled model will likely be further away from the local reality than the individual component models forced by observations. For example, forced by the observed climatology of the Arabian Peninsula, the offline vegetation model simulates a desert. When a desert is imposed in the peninsula, the climate model simulates a limited monsoon over the region. In the coupled vegetation-climate model, the vegetation responds to the monsoonal rain, resulting in more extensive rainfall over the peninsula. Coupling models with each other is thus not likely to correct the biases of the individual models: the biases can be enhanced or damped by the coupling but in the latter case most likely not for the right reason. When coupling models with each other, modelers need to understand the origin of the individual biases in order to know what result of they can trust in the coupled model. Following from these points, modelers should probably test the validity of a coupled model against the results of the individual components as well as against observations.

Acknowledgements

We thank Mike Coe, Simon Donner, Chris Kucharik, and Navin Ramankutty for useful comments on earlier drafts of this manuscripts.

Figure Legends

Figure 1: Schematic representation of the carbon cycle in IBIS.

Figure 2: (a) Difference between temperatures simulated by the coupled model at the lowest GCM level (between surface and 65 meters) and observed temperatures from the CRU05 climatology [New *et al.*, 2000] for December, January, February, and (b) June, July, August. (c) Difference between precipitation simulated by the coupled model and observed precipitation from the CRU05 climatology for December, January, February, and (d) June, July, August.

Figure 3: Distribution of potential leaf area index of evergreen trees, deciduous trees, and grasses and shrubs simulated by the offline model forced with the CRU05 climate and simulated by the coupled model.

Figure 4: Distribution of potential vegetation types simulated by the offline model forced with the CRU05 climate and simulated by the coupled model.

Figure 5: Distribution of biomass (kg C m^{-2}), simulated by the offline model and by the coupled model.

Figure 6: Distribution of soil carbon content (kg C m^{-2}) to a depth of 1 m, simulated by the offline model and by the coupled model.

Figure 7: Soil carbon content (kgC m^{-2}) averaged per vegetation type (± 1 standard deviation) as observed (IGBP-DIS,1999), simulated by the offline model and by the coupled model. The standard deviations in the model results and observations represent variations within each vegetation type.

Figure 8: Zonal totals of annual average net primary productivity, NPP (Gt C yr^{-1}), heterotrophic respiration, HR, and disturbance. The dotted lines are results from the offline model and the plain lines are results from the coupled model.

Figure 9: Annual net primary productivity (NPP in $\text{kg C m}^{-2} \text{ yr}^{-1}$) averaged per vegetation type (± 1 standard deviation) as observed (Gower, unpublished data, 1999), simulated by the offline model and by the coupled model. The standard deviations in the model results and observations represent variations within each vegetation type.

Figure 10: Average seasonal cycle of NPP (squares), heterotrophic respiration (circles), net ecosystem exchange (triangles) aggregated over 30° latitude bands. The dotted lines indicate results from the offline model, plain lines results from the coupled model. The seasonal cycles are presented as anomalies from the annual means.

Figure 11: Average seasonal cycle of zonal mean (a) NPP, (b) heterotrophic respiration, and (c) net ecosystem exchange simulated by the offline model (top panel), the coupled model (middle panel) and the difference between the coupled and the offline model (bottom panel). The seasonal cycles are presented as anomalies from the annual means. The dotted (plain) contours indicate negative (positive) anomalies.

References.

- Amthor, J.S., The role of maintenance respiration in plant growth, *Plant, cell and environment*, 7, 561-569, 1984.
- Bonan, G.B., The land surface climatology of the NCAR Land Surface Model coupled to the NCAR Community Climate Model, *Journal of Climate*, 11 (6), 1307-1326, 1998.
- Botta, A., and J.A. Foley, Effects of Climate Variability and Disturbances on the Amazonian Terrestrial Ecosystems Dynamics., *Global Biogeochemical Cycles*, June 2002, In press.
- Botta, A., N. Viovy, P. Ciais, P. Friedlingstein, and P. Monfray, A global prognostic scheme of leaf onset using satellite data, *Global Change Biology*, 6 (7), 709-725, 2000.
- Cannell, M.G.R., *World Forest Biomass and Primary Production Data*, 375 pp., Academic Press, London, 1982.
- Collatz, G.J., M. Ribas-Carbo, and J.A. Berry, Coupled photosynthesis-stomatal conductance model for leaves of C₄ plants, *Australian Journal of Plant Physiology*, 19, 519-538, 1992.
- Collatz, J.G., J.T. Ball, C. Grivet, and J.A. Berry, Physiological and environmental regulation of stomatal conductance, photosynthesis and transpiration: a model that includes a laminar boundary layer, *Agricultural and Forest Meteorology*, 53, 107-136, 1991.

- Cox, P.M., R.A. Betts, C.D. Jones, S.A. Spall, and I.J. Totterdell, Acceleration of global warming due to carbon-cycle feedbacks in a coupled climate model (vol 408, pg 184, 2000), *Nature*, 408 (6813), 750-750, 2000.
- Craig, S.G., K.J. Holmen, G.B. Bonan, and P.J. Rasch, Atmospheric CO₂ simulated by the National Center for Atmospheric Research Community Climate Model - 1. Mean fields and seasonal cycles, *Journal of Geophysical Research-Atmospheres*, 103 (D11), 13213-13235, 1998.
- Cramer, W., D.W. Kicklighter, A. Bondeau, B. Moore, C. Churkina, B. Nemry, A. Ruimy, and A.L. Schloss, Comparing global models of terrestrial net primary productivity (NPP): overview and key results, *Global Change Biology*, 5, 1-15, 1999.
- Delire, C., and J.A. Foley, Evaluating the performance of a land Surface/ecosystem model with biophysical measurements from contrasting environments, *Journal of Geophysical Research-Atmospheres*, 104 (D14), 16895-16909, 1999.
- Delire, C., S.L. Levis, G. Bonan, J.A. Foley, M.T. Coe, and S. Vavrus, Comparison of the climate simulated by the CCM3 coupled to two different land-surface models., *Climate Dynamics*, in press June 2002.
- Denning, A.S., G.J. Collatz, C. Zhang, D.A. Randall, J.A. Berry, P.J. Sellers, G.D. Colello, and D.A. Dazlich, Simulations of terrestrial carbon metabolism and atmospheric CO₂ in a general circulation model Part 1: surface carbon fluxes, *Tellus*, 48B, 521-542, 1996.

- Esser, G., H.F.H. Lieth, J.M.O. Scurlock, and R.J. Olson, Worldwide estimates and bibliography of net primary productivity derived from pre-1982 publications, pp. 104, Oak Ridge Nat. Lab., Oak Ridge, Tenn., 1997.
- Farquhar, G.D., S. von Caemmerer, and J.A. Berry, A biochemical model of photosynthetic CO₂ assimilation in leaves of C₃ species, *Planta*, 149, 78-90, 1980.
- Foley, J.A., S. Levis, M.H. Costa, W. Cramer, and D. Pollard, Incorporating dynamic vegetation cover within global climate models, *Ecological Applications*, 10 (6), 1620-1632, 2000.
- Foley, J.A., S. Levis, I.C. Prentice, D. Pollard, and S.L. Thompson, Coupling dynamic models of climate and vegetation, *Global Change Biology*, 4 (5), 561-579, 1998.
- Foley, J.A., I.C. Prentice, N. Ramankutty, S. Levis, D. Pollard, S. Sitch, and A. Haxeltine, An integrated biosphere model of land surface processes, terrestrial carbon balance, and vegetation dynamics, *Global Biogeochemical Cycles*, 10 (4), 603-628, 1996.
- Friedlingstein, P., L. Bopp, P. Ciais, J.L. Dufresne, L. Fairhead, H. LeTreut, P. Monfray, and J. Orr, Positive feedback between future climate change and the carbon cycle, *Geophysical Research Letters*, 28 (8), 1543-1546, 2001.
- Fung, I.Y., C.J. Tucker, and K.C. Prentice, Application of advanced very high resolution radiometer vegetation index to study atmosphere-biosphere exchange of CO₂, *Journal of Geophysical Research*, 92 (D3), 2999-3015, 1987.
- Gates, W.L., Climate models-evaluation, in *IPCC*, 1995.

- Gower, S.T., C.J. Kucharik, and J.M. Norman, Direct and indirect estimation of leaf area index, $f(\text{APAR})$, and net primary production of terrestrial ecosystems, *Remote Sensing of Environment*, 70 (1), 29-51, 1999.
- Holdridge, L.R., Determination of world plant formations from simple climatic data, *Science*, 105, 367-368, 1947.
- IGBP-DIS, Global Soil Data Task: Spatial Database of Soil Properties, International Geosphere-Biosphere Programme - Data and Information System, Toulouse, France, 1999.
- Kiehl, J.T., J.J. Hack, G.B. Bonan, B.A. Boville, D.L. Williamson, and P.J. Rasch, The National Center for Atmospheric Research Community Climate Model: CCM3, *Journal of Climate*, 11 (6), 1131-1149, 1998.
- Knorr, W., and M. Heimann, Impact of Drought Stress and Other Factors on Seasonal Land Biosphere Co₂ Exchange Studied through an Atmospheric Tracer Transport Model, *Tellus Series B-Chemical and Physical Meteorology*, 47 (4), 471-489, 1995.
- Kucharik, C.J., J.A. Foley, C. Delire, V.A. Fisher, M.T. Coe, J.D. Linters, C. Young-Molling, N. Ramankutty, J.M. Norman, and S.T. Gower, Testing the performance of a Dynamic Global Ecosystem Model: Water balance, carbon balance, and vegetation structure, *Global Biogeochemical Cycles*, 14 (3), 795-825, 2000.
- Linters, J.D., M.T. Coe, and J.A. Foley, Surface water balance of the continental United States, 1963- 1995: Regional evaluation of a terrestrial biosphere model and the NCEP/NCAR reanalysis, *Journal of Geophysical Research-Atmospheres*, 105 (D17), 22393-22425, 2000.

- Levis, S., J.A. Foley, V. Brovkin, and D. Pollard, On the stability of the high-latitude climate-vegetation system in a coupled atmosphere-biosphere model, *Global Ecology and Biogeography*, 8 (6), 489-500, 1999a.
- Levis, S., J.A. Foley, and D. Pollard, CO₂, climate, and vegetation feedbacks at the Last Glacial Maximum, *Journal of Geophysical Research-Atmospheres*, 104 (D24), 31191-31198, 1999b.
- Levis, S., J.A. Foley, and D. Pollard, Potential high-latitude vegetation feedbacks on CO₂-induced climate change, *Geophysical Research Letters*, 26 (6), 747-750, 1999c.
- Levis, S., J.A. Foley, and D. Pollard, Large-scale vegetation feedbacks on a doubled CO₂ climate, *Journal of Climate*, 13 (7), 1313-1325, 2000.
- Lieth, H., Modeling the primary productivity of the world, in *Primary Productivity of the Biosphere*, edited by H. Leith, and R.H. Whittaker, pp. 237-263, Springer-Verlag, New York, 1975.
- Monserud, R.A., Methods for comparing Global Vegetation Maps, pp. 31, International Institute for Applied Systems Analysis, Laxenburg, Austria, 1990 (Aug).
- Nemry, B., L. Francois, P. Warnant, F. Robinet, and J.C. Gerard, The seasonality of the CO₂ exchange between the atmosphere and the land biosphere: A study with a global mechanistic vegetation model, *Journal of Geophysical Research-Atmospheres*, 101 (D3), 7111-7125, 1996.
- New, M., M. Hulme, and P. Jones, Representing twentieth-century space-time climate variability. Part II: Development of 1901-96 monthly grids of terrestrial surface climate, *Journal of Climate*, 13 (13), 2217-2238, 2000.

- Parton, W.J., J.M.O. Scurlock, D.S. Ojima, T.G. Gilmanov, R.J. Scholes, D.S. Schimel, T. Kirchner, J.-C. Menaut, T. Seastedt, E. Garcia Moya, A. Kamnalrut, and J.I. Kinyamario, Observations and modeling of biomass and soil organic matter dynamics for the grassland biome worldwide, *Global Biogeochemical Cycles*, 7 (4), 785-809, 1993.
- Post, W.M., W.R. Emanuel, P.J. Zinke, and A.G. Stangenberger, Soil carbon pools and world life zones, *Nature*, 298, 156-159, 1982.
- Ramankutty, N., and J.A. Foley, Estimating historical changes in global land cover: Croplands from 1700 to 1992, *Global Biogeochemical Cycles*, 13 (4), 997-1027, 1999.
- Scholes, R.J., D. Skole, and J.S. Ingram, A global database of soil properties: Proposal for implementation, GCTE Focus 3 Associate Office, Oxford, UK, 1995.
- Thompson, S.L., and D. Pollard, A global climate model (genesis) with a land-surface transfer scheme (lsx). Part II: CO₂ sensitivity, *Journal of Climate*, 8 (5), 1104-1121, 1995a.
- Thompson, S.L., and D. Pollard, A global climate model (GENESIS) with a land-surface-transfer scheme (LSX). Part I: Present-day climate, *J. Climate*, 8, 732-761, 1995b.
- Verberne, E.L.J., J. Hassink, P. Dewilligen, J.J.R. Groot, and J.A. Vanveen, Modeling Organic-Matter Dynamics in Different Soils, *Netherlands Journal of Agricultural Science*, 38 (3), 221-238, 1990.

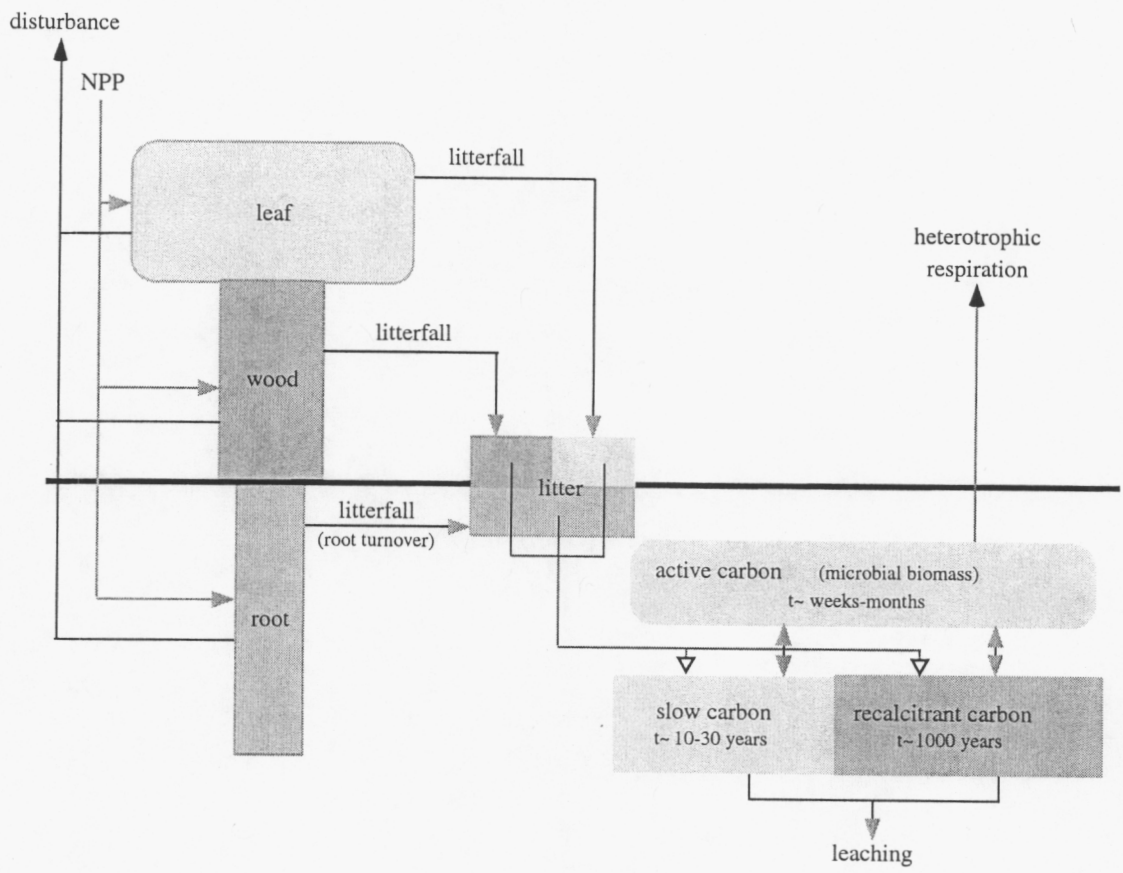


Figure 1

a) Coupled model minus climatology, temperature, DJF c) Coupled model minus climatology, precipitation (mm/day), DJF



b) Coupled model minus climatology, temperature, JJA d) Coupled model minus climatology, precipitation (mm/day), JJA



Figure 2

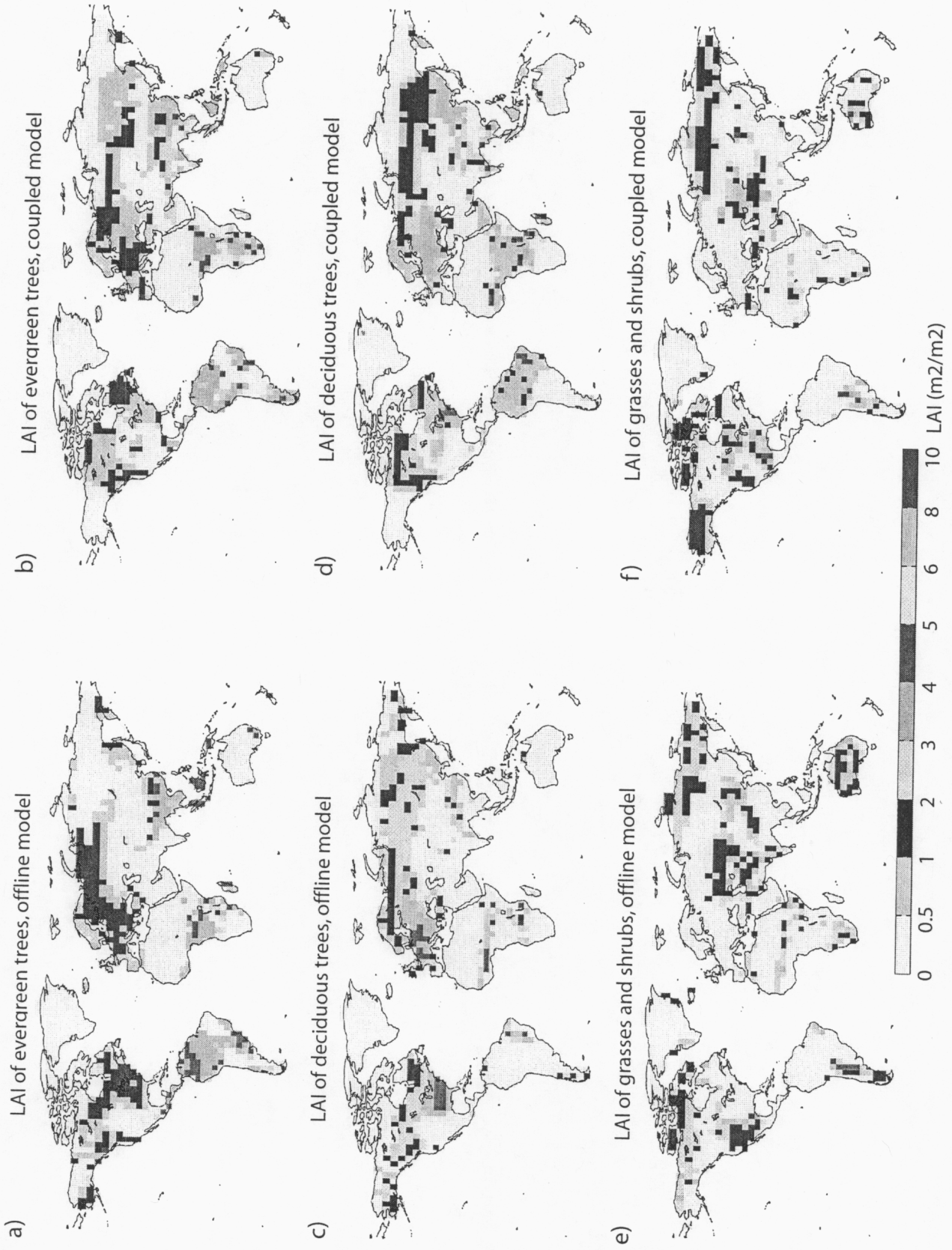
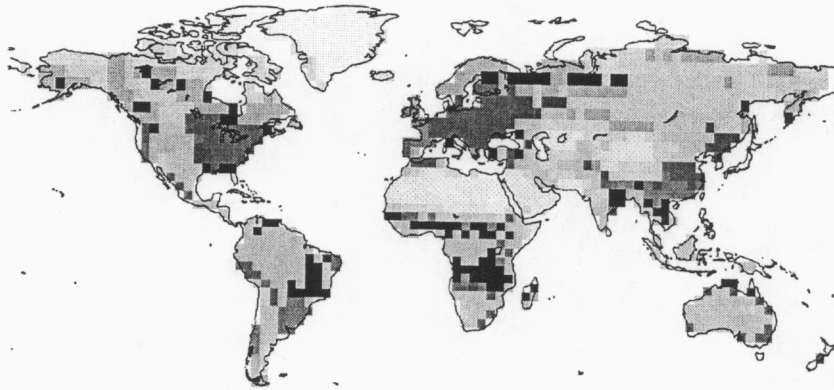


Figure 3

Vegetation types, offline model



Vegetation types, coupled model

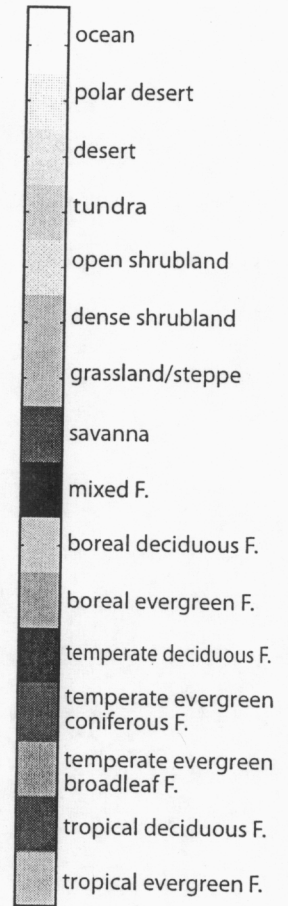
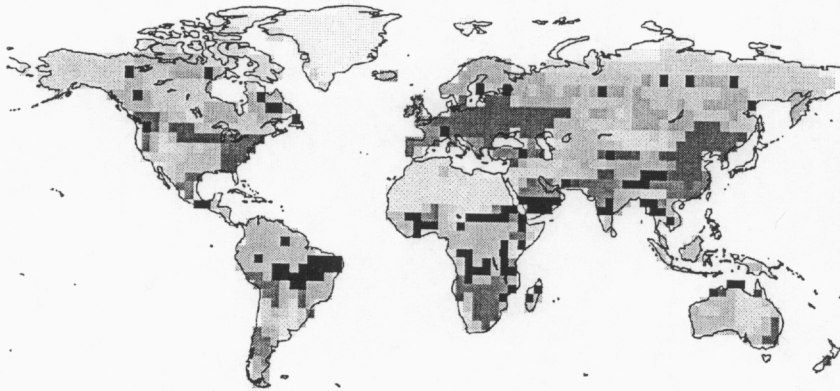


Figure 4

Biomass (kg C m⁻²), offline model.



Biomass (kg C m⁻²), coupled model.

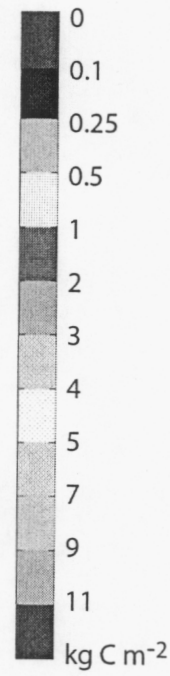
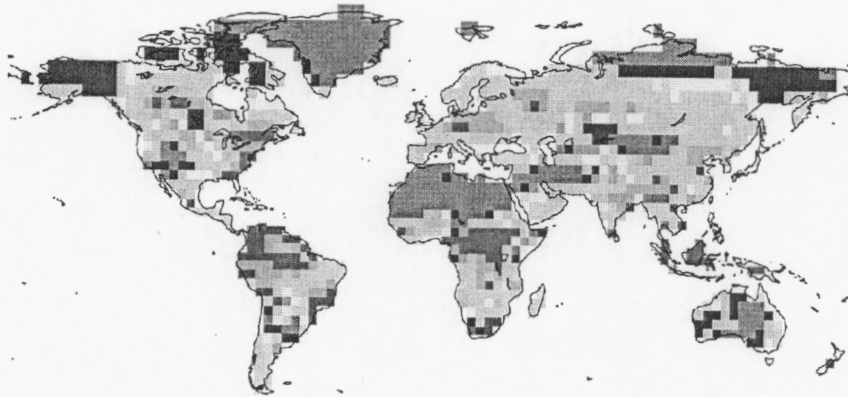
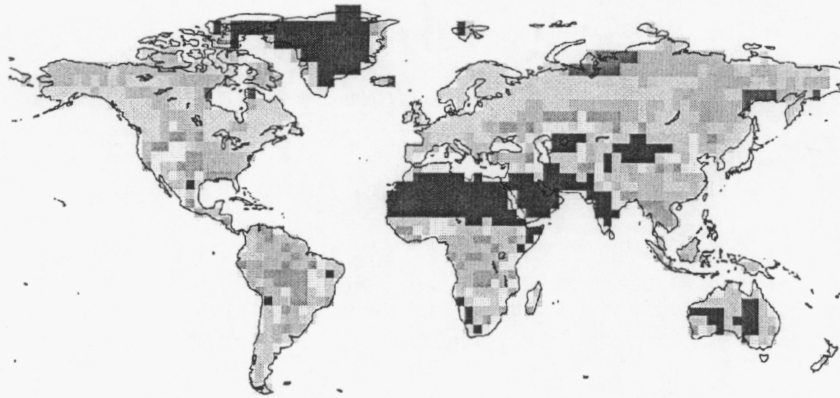


Figure 5

Total Soil Carbon Content (kg C m⁻²), offline model



Total Soil Carbon Content (kg C m⁻²), coupled model

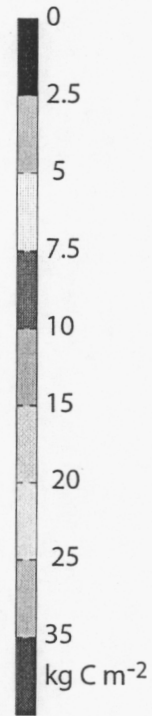
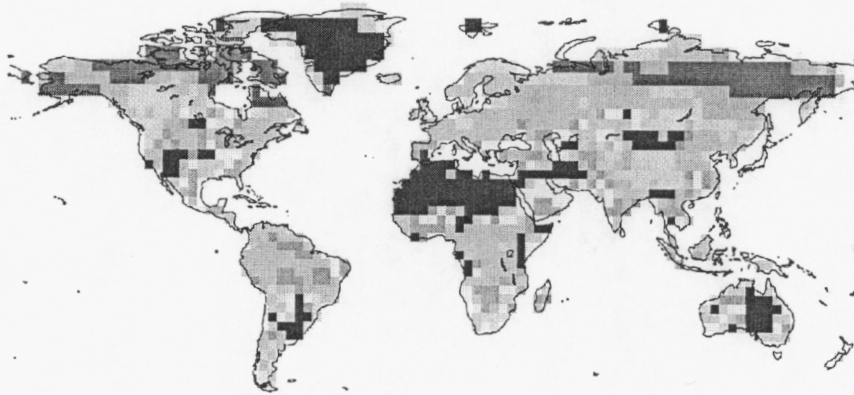


Figure 6

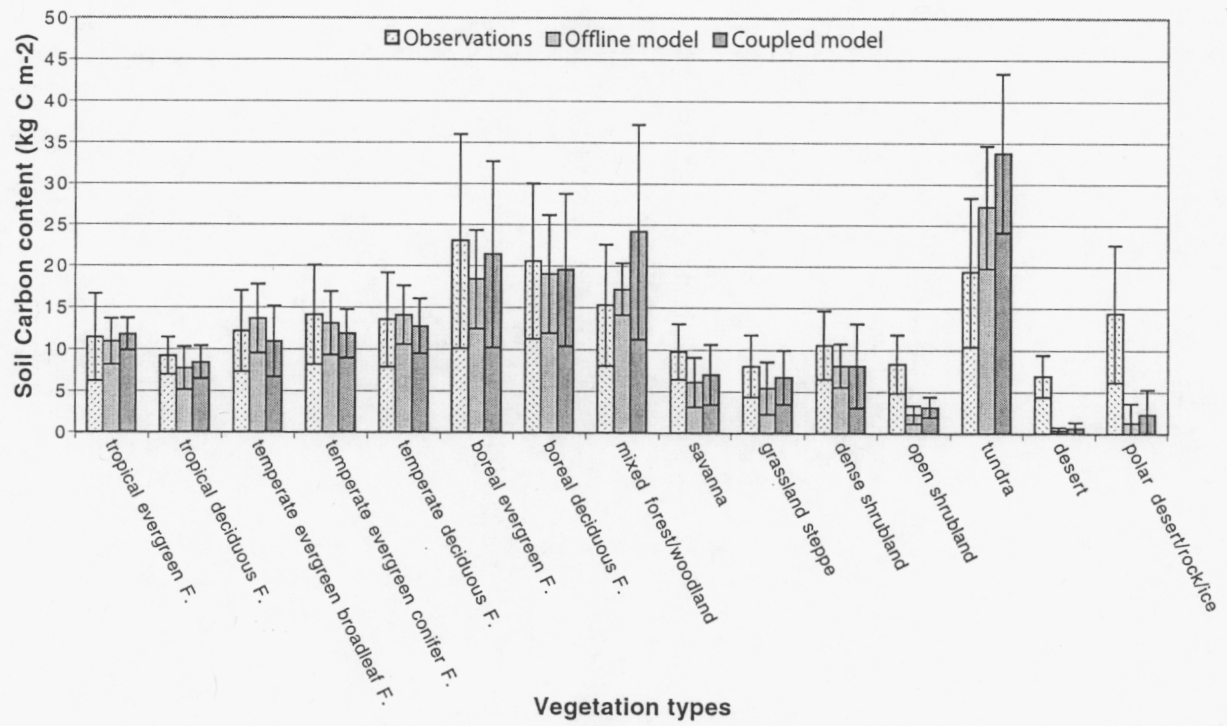


Figure 7

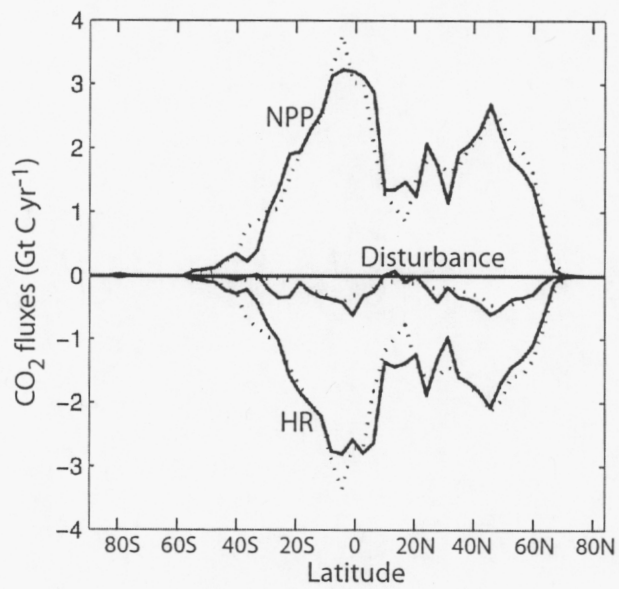


Figure 8

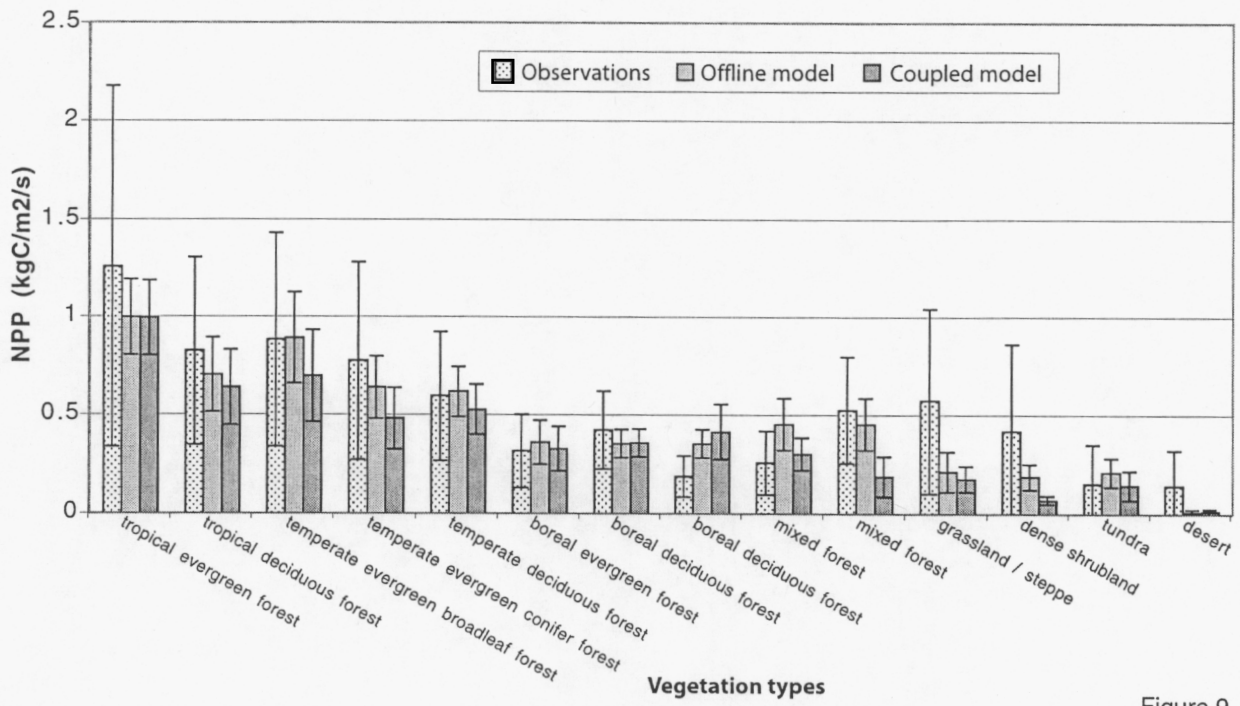


Figure 9

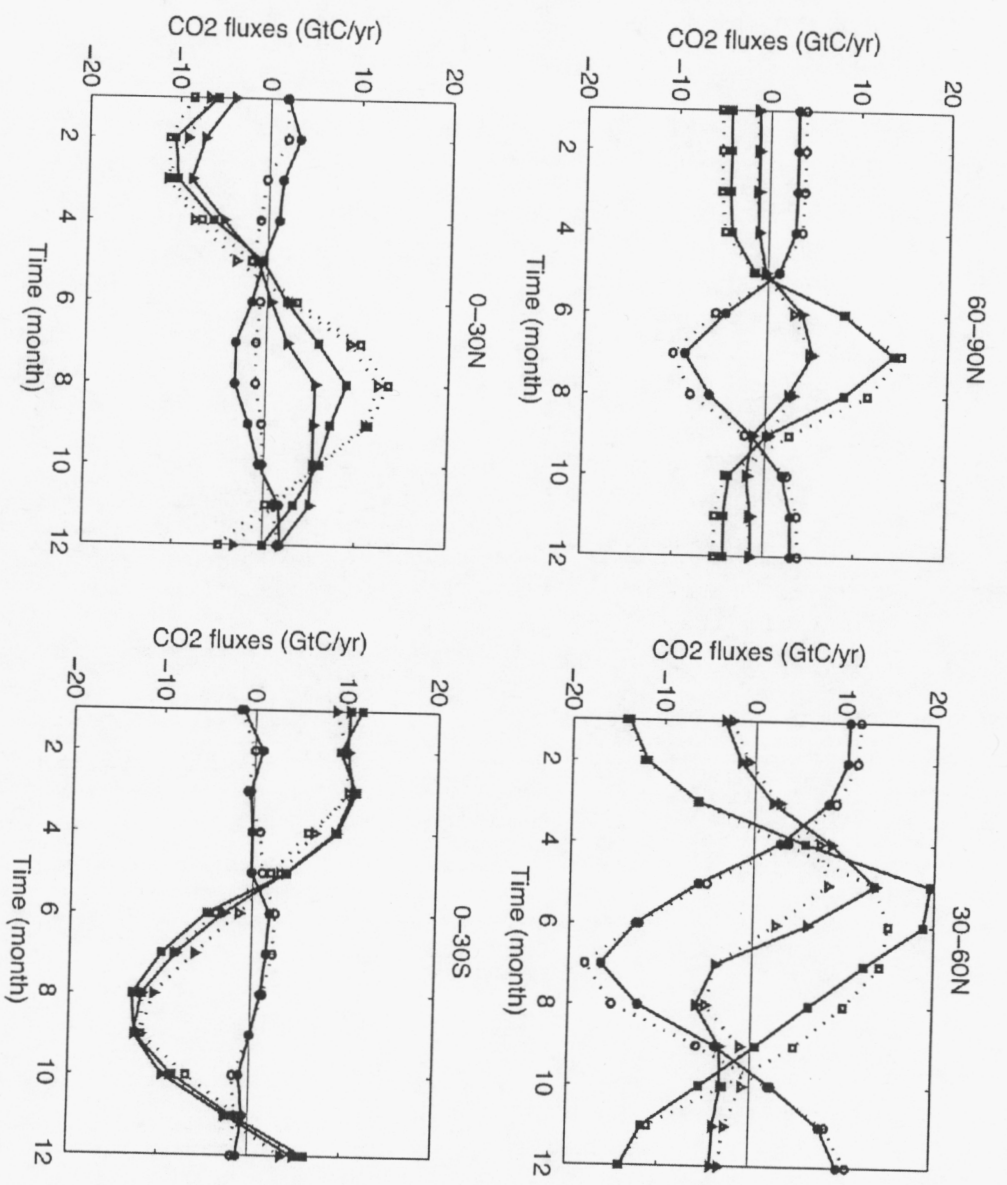


Figure 10

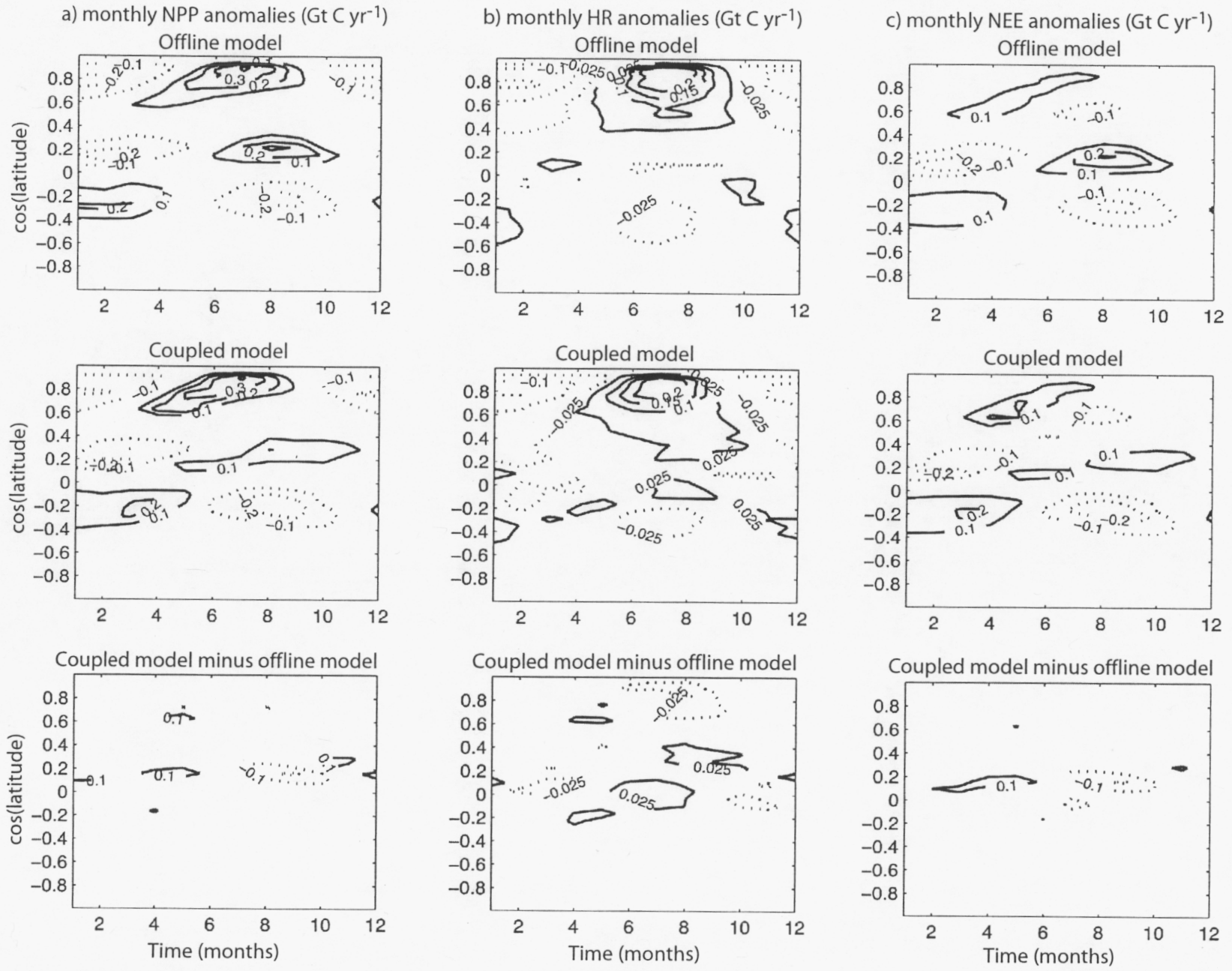


Figure 11